SHOT NOISE LIMITS TO SENSITIVITY OF OPTICAL INTERFEROMETRY

Sudhakar Prasad

Center for Advanced Studies & Dept. of Physics and Astronomy
University of New Mexico, Albuquerque NM 87131

Abstract

By arguing that the limiting noise is the photoelectron shot noise, we show that the sensitivity of image synthesis by an ideal optical interferometer is *independent* of the details of beam-splitting and recombination. The signal-to-noise ratio of the synthesized image is proportional to the square root of the total number of photoelectrons detected by the entire array. For non-ideal interferometers, which are forced to employ a closure-phase method of indirect inference of the visibility data, essentially the same result holds for strong sources, but at weak light levels beam-splitting degrades sensitivity.

Section I: Introduction

A major distinction between synthetic aperture imaging of astronomical objects at radio and at optical frequencies is that for the former the wave noise dominates the photon counting noise while for the latter the reverse holds. This is especially significant since in the optical domain noise-free amplification of the photon number does not seem possible and thus the photon counting noise cannot be reduced simply by amplification. Furthermore, modern photoelectric detectors do not suffer from significant dark currents or other sources of instrument noise. In other words, the sensitivity of optical imaging via aperture synthesis is limited principally by photoelectron shot noise, which is determined solely by the strength of the source and the collecting area of the array.

Here, we have analyzed the signal-to-noise ratio (SNR) and the distribution of noise across the image plane of an optical aperture synthesis array, and the dependence of these quantities on the beam combination geometry. The aperture synthesis method employs the van Cittert-Zernike theorem (Goodman 1985), which states that the object intensity is the two-dimensional Fourier transform of the distribution of spatial coherence in a plane. For a given total collecting area spread over n apertures, there are many different ways of experimentally deducing the spatial

correlation of the light field on the available $n_b \equiv n(n - 1)/2$ baselines. The different ways correspond to how the original beams are first split and then recombined. For example, one could split each of the original n beams into ${}^{n-1}C_{r-1}$ sub-beams and recombine r different sub-beams at a time on ${}^{n}C_{r}$ different detectors. We shall henceforth call such an array an ${}^{n}C_{r}$ array. The two extreme cases of the ${}^{n}C_{r}$ array are the ${}^{n}C_{2}$ array, in which the fringes corresponding to the n_b individual baselines fall on n_b separate detectors, and the ${}^{n}C_{n}$ array, in which *all* fringes for all baselines fall on a *single* detector. We have analyzed only these two arrays and found that the sensitivity depends only slightly on the details of beam combination. The SNR is found, up to factors of order 1, to be $\sqrt{L}$ where L is the total number of photoelectrons collected by the entire array in the integration time.

Unlike space-based and lunar optical arrays, ground-based arrays are afflicted by the atmospheric phase corruption of astronomical signals. Ground-based arrays thus suffer not only from the photon shot noise but from the more important phase noise of the atmosphere, a fact that forces them to employ a closure-phase method (Baldwin *et al.* 1986) of recovery of spatial coherence data analogous to that in the radio domain (Pearson and Readhead 1984). We have also computed in this report the SNR of the bispectrum, whose phase is the closure phase, for an ${}^{n}C_{2}$ array.

Our work concerns only the analysis of noise coming from the detection of individual fringe phasors, not the noise arising from an incomplete sampling of the spatial frequency plane, since the latter is well understood. In this report we shall only present the most salient results, since these and several others will be derived in detail in a series of papers (Prasad and Kulkarni 1989, Kulkarni, Prasad, and Nakajima *in preparation*) to be published.

Section II: An Ideal ${}^{n}C_{2}$ Interferometer

Let there be n identical principal apertures from which we derive n main beams. Each main beam is divided into n - 1 identical sub-beams by the use of beam splitters. The resulting $n(n-1)$ sub-beams are combined pairwise on $n_b = {}^{n}C_{2}$ identical detectors, each with P pixels. Each detector may thus be identified with one spatial frequency, or baseline. The average photoelectron counts at the pixel $\vec{p}$ of the rth detector is proportional to the average intensity at that pixel and may be written as

$$\langle k_r(p) \rangle = 2\langle K_0 \rangle [1 + \gamma_r \cos(p\omega_r + \phi_r)], \qquad (2.1)$$

where $\gamma_r e^{i\phi_r}$ is the complex visibility, or spatial coherence, for spatial frequency $\vec{\omega}_r$. Here, <...> refers to averaging over the photoelectron detection process. The product $p\omega_r$ is to be understood as the scalar product of the pixel position vector $\vec{p}$ and the spatial frequency $\vec{\omega}_r$ expressed in inverse pixel units. If $<C>$ is the average number of photoelectrons detected by the entire array in one integration period, then $2<N> \equiv <C>/n_b$ is the average number of photoelectrons per detector in that period. From equation (2.1), the average number of photoelectrons per detector is equal to $2<K_0>P$ and thus $<K_0>P = <N>$.

Each detector yields two fringe phasors: z_r, the spatial frequency component corresponding to the baseline r, and z_r^0, the photoelectron count or the zero spatial frequency component derived from the fringe pattern on that detector. These quantities are operationally defined by the relations

$$z_r = \sum_{p=1}^{P} k_r(p)\, e^{-ip\omega r}, \quad z_r^0 = \sum_{p=1}^{P} k_r(p)\,. \tag{2.2}$$

Throughout this article we will use the upper case for the ensemble average of a random variable. There are two different ways by which the synthesized image can be constructed from the visibility data: The first uses only the nonzero spatial frequencies in inversion ("inversion without total photocounts"), while the second uses *all* frequencies including z_r^0 ("true inversion"). Despite the fact that the first method produces *zero* total photon number in the map, it is the standard method in radio astronomy.

We now discuss for the two methods of noise distribution in the maps due to the statistical nature of the photoelectric detection process, which limits the accuracy with which fringe phasors may be measured via relations of kind (2.2). The statistics of the shot noise are Poissonian on account of which the variance in the photoelectron count in pixel p is equal to the average photoelectron count $<k(p)>$. In contrast to the sampling errors, which may be CLEANed away (see, e.g., Perley, Schwab, and Bridle 1985), there is no technique by which the effects of shot noise can be reduced. In what follows, we analyze the effect of shot noise on the maximum achievable SNR in the synthesized map.

a. Inversion Without Total Counts. The synthesized image is the real portion of the Fourier transform of the spatial coherence function. On pixel q in the image, its value is

$$i_1(q) \equiv \mathrm{Re} \sum_{r=1}^{n_b} z_r e^{iq\omega r}. \tag{2.3a}$$

The mean map $I_1(q)$ is given by

$$I_1(q) = \langle N \rangle \sum_r \gamma_r \cos(\omega_r q + \phi_r). \tag{2.3b}$$

The image $I_1(q)$ may be referred to as the "dirty image," since it suffers from errors caused by incomplete sampling of the spatial frequency plane. A synthesized image can be obtained from the dirty image by any one of the popular deconvolution techniques (see Perley, Schwab, and Bridle 1985).

The variance $V[i_1(q)]$ in the synthesized map $i_1(q)$ will clearly involve three kinds of covariances: cov[Re(z_r), Re(z_s)], cov[Re(z_r), Im(z_s)], and cov[Im(z_r), Im(z_s)]. Since there is no correlation of the photoelectron shot noise between different detectors or between different pixels of the same detector, and since shot noise has Poisson statistics, one may show that

$$\mathrm{cov}[\mathrm{Re}(z_r),\mathrm{Re}(z_s)] = \mathrm{cov}[\mathrm{Im}(z_r), \mathrm{Im}(z_s)] = \langle N \rangle \delta_{rs}, \tag{2.4}$$

while cov[Re(z_r), Im(z_s)] = 0. After some algebra, the variance $V[i_1(q)]$ in the map turns out to be half the total number of photoelectrons intercepted by the entire array: $V[i_1(q)] = \langle C \rangle/2$. Furthermore, the variance *is independent of the pixel position as well as the object structure.* This is certainly a desirable feature of any aperture synthesis technique.

For the specific case of a point source ($\gamma_r = 1$) at the phase center ($\phi_r = 0$), the central pixel in the image, which is indicative of the entire map, has the mean value $I_1(0) = (\langle C \rangle/2)$ and hence the SNR

$$\frac{I_1(0)}{\sqrt{V\,[i_1(0)]}} = \sqrt{\frac{\langle C \rangle}{2}} \quad . \tag{2.5}$$

Indeed, apart from the factor of $\sqrt{1/2}$, this is the SNR expected physically. This variance refers to the image obtained by synthesizing one *single* set of measurements of the n_b phasors. If the measurements were repeated m times then both the image and the variance would be scaled up by m and the SNR in the resulting map would be $\sqrt{<L>/2}$ where $L = <C>m$ is the total number of photoelectrons intercepted by the array over the m coherent integration intervals.

b. <u>True Inversion</u>. According to the van Cittert-Zernike theorem, *all* the spatial frequency components must be used to construct the images. In our inversion, we include only *positive* nonzero spatial frequencies as in equation 2.3*a*. This is a valid procedure, since the corresponding *negative* frequency components are merely their complex conjugates. Thus the zero spatial frequency phasor, which is its own complex conjugate, must be *halved* (or equivalently, all the positive frequency terms *doubled*) before it is included in such an inversion procedure, one that suppresses all nonzero spatial frequencies of one sign. The synthesized image is then specified by

$$i_2(q) \;=\; i_1(q) + \frac{1}{2}\sum_r z_r^0 , \tag{2.6a}$$

the mean value of which is

$$I_2(q) = \langle N \rangle \sum_r [\gamma_r \cos(\phi_r + \omega_r q) + 1] = I_1(q) + \frac{\langle C \rangle}{2} , \tag{2.6b}$$

which is nonnegative for all q since $\gamma_r \cos(\phi_r + \omega_r q) + 1$ is so for all r.

As before, we estimate the variance due to the shot noise of the detection process. From equation 2.6*a* it is clear that $V[i_2(q)]$ differs from $V[i_1(q)]$ by terms containing covariances that involve z_r^0. We shall skip the details of the straightforward algebra and only give the final result:

$$V\,[i_2(q)] = \frac{3}{4}\langle C \rangle + I_1(q) = \frac{\langle C \rangle}{4} + I_2(q) . \tag{2.7}$$

Thus unlike the previous method the variance is no longer uniform across the map, being composed of a fixed amount ($<C>/4$) and a variable amount *equal to the dirty image*. Physically this is so since the zero spatial frequency components are highly correlated with the corresponding fringe phasors. This is a general result valid in the radio domain as well (Kulkarni 1989), where at low source strength the fringe phasors are uncorrelated while at high source strength they are correlated. Correspondingly, in the first case the variance is uniform while in the second case it is not.

Again for a point source at the phase center, $\gamma_r = 1$ and $\phi_r = 0$, the mean central pixel in the map is $I_2(0) = <C>$ and the corresponding SNR is $\sqrt{8/5}\ \sqrt{<C>/2}$, which represents an enhancement by a factor $F = \sqrt{8/5}$ over the previous case. Henceforth, we refer to F as the "enhancement factor," using it as some kind of figure of merit. Thus, inclusion of the zero spatial frequency improves the SNR but at the expense of a nonuniform variance.

Section III: Ideal ${}^nC_n$ Interferometers

In an ${}^nC_n$ interferometer, all the n_b different fringes lie on top of each other on a single detector. Although equation (2.2) may be used to recover each of the n_b fringe phasors individually, one expects, at first glance, the image synthesis to be rather noisy, since the different fringe phasors are not all uncorrelated. However, our careful analysis proves otherwise and provides, at the same time, insight into improved schemes of imaging. We consider first an ${}^nC_n$ interferometer with no redundancy of baselines and then an ${}^nC_n$ interferometer with maximum possible redundancy. The redundancy of baselines is not of much significance for lunar or space-based arrays, except insofar as it inhibits a rapid coverage of the spatial-frequency plane. We consider both cases because a lot of analytical simplifications that are possible in the former are invalid in the latter. However, we show that in either case the SNR in the map is roughly the same and, in fact, approximately equal to that of an ${}^nC_2$ interferometer.

a. A Fully Nonredundant Mask. Let us consider the general case of a nonredundant mask of n identical apertures, labeled by lower-case roman letters, being illuminated by a source. The classical intensity distribution of the interference pattern by the n apertures translates into the following form for the average photocounts at pixel p of the detector:

$$\langle k(p)\rangle = \langle Q_0\rangle \left[n + 2 \sum_{g<h=1}^{n} \gamma_{gh} \cos(p\omega_{gh} + \phi_{gh}) \right]. \qquad (3.1)$$

Here $<Q_0>$ has pretty much the same meaning as K_0 in Section II. However, since there is no beam splitting, $<Q_0> = (n\text{-}1)<K_0>$.

As before, we need to compute the means, variances, and covariances of the fringe phasors, z_{ij}, to estimate the variance in the synthesized image. The mean phasor on the ij baseline (i.e., the baseline connecting aperture i to aperture j) is given by

$$Z_{ij} = \langle Q_0 \rangle \sum_p e^{-ip\omega_{ij}} \left[n + 2 \sum_{g<h} \gamma_{gh} \cos(p\omega_{gh} + \phi_{gh}) \right], \qquad (3.2)$$

while the covariance, of say the real parts of two fringe phasors z_{ij} and $z_{k\ell}$, is given by

$$\begin{aligned} \mathrm{cov}[\mathrm{Re}(z_{ij}), \mathrm{Re}(z_{k\ell})] &= \sum_p \langle k_p \rangle \cos(p\omega_{ij}) \cos(p\omega_{k\ell}) \\ &= \langle Q_0 \rangle \sum_p [n + 2 \sum_{g<h} \gamma_{gh} \cos(p\omega_{gh} + \phi_{gh})] \cos(p\omega_{ij}) \cos(p\omega_{k\ell}). \end{aligned} \qquad (3.3.)$$

By writing every cosine as a sum of two exponentials, we have terms in (3.2) and (3.3) that involve all possible combinations of two and three spatial frequencies $\pm\omega_{ij} \pm \omega_{k\ell}$ and $\pm\omega_{gh} \pm \omega_{ij} \pm \omega_{k\ell}$. Contributions from the pixel sum survive only when these frequency combinations vanish. We now impose two nonredundancy conditions on the array: (*i*) "nonredundancy of baselines," which requires that $\omega_{ij} \neq \pm\omega_{k\ell}$ aunless (ij) and (gh) refer to the same baseline and (*ii*) "nonredundancy of triangles," which requires that

$$\omega_{gh} \pm \omega_{ij} \pm \omega_{k\ell} \neq 0, \tag{3.4}$$

unless (gh), (ij), and $(k\ell)$ form the sides of a triangle. Thus while the first condition maximally constrains the baselines or vectors in any array, the second condition imposes the maximal nonredundancy condition on triangles. As before, we shall only summarize results. The reader is referred to our paper (Prasad and Kulkarni 1989) for details.

(i) Inversion Without Total Counts. Following the formulation in Section II*a* we find the mean synthesized image to be

$$\langle I_3(q) \rangle = \langle M \rangle \sum_{i<j} \gamma_{ij} \cos(q\omega_{ij} + \phi_{ij}). \tag{3.5}$$

To evaluate the variance, we first expand it in terms of the covariances of the individual fringe phasors. After long algebra, one obtains the following final expression:

$$V\,[i_3(q)] = \frac{\langle M \rangle}{2} \left[n\,n_b + 2(n-2) \sum_{i<j} \gamma_{ij} \cos(q\omega_{ij} + \phi_{ij}) \right]. \tag{3.6}$$

The variance consists of a constant component n_b $<C>/2$ and a comparable variable component. The latter disappears for n=2, in consistency with the results of Section II. For a point source at the phase center for which $\gamma_{ij} = 1$ and $\phi_{ij} = 0$, the SNR of the central pixel turns out to be

$$\frac{I_3(0)}{\sqrt{V\,[i_3(0)]}} = \sqrt{\frac{\langle C \rangle}{2}} \sqrt{\frac{2n-2}{3n-4}}. \tag{3.7}$$

The enhancement factor $F = \sqrt{(2n-2)/(3n-4)}$ is unity for n=2 and steadily decreases to $\sqrt{2/3}$ as the number of apertures increases. Thus this interferometer is not quite as efficient as the ${}^nC_2$ interferometer.

(ii) True Inversion. The mean and the variance of the map constructed by including z_0 are given by appending to equations (3.5) and (3.6) terms that arise from the inclusion of z_0 in the Fourier inversion. One has

$$I_4(q) = \langle M \rangle \left[\frac{n}{2} + \sum_{i<j} \gamma_{ij} \cos(q\omega_{ij} + \phi_{ij}) \right] \tag{3.8}$$

and

$$V\,[i_4(q)] = \frac{\langle M \rangle}{2} \left[n\,(\frac{1}{2} + n_b) + 2(n-1) \sum_{i<j} \gamma_{ij} \cos(q\omega_{ij} + \phi_{ij}) \right] . \tag{3.9}$$

Clearly even for n=2, a single nontrivial baseline, the variance is not uniform throughout the map. However, the SNR at the map center for a point source ($\gamma_{ij} = 1$, $\phi_{ij} = 0$).

$$\frac{I_4(0)}{\sqrt{V\,[i_4(0)]}} = \sqrt{\frac{\langle C \rangle}{2}} \sqrt{\frac{2n^2}{3n^2 - 5n + 3}} , \tag{3.10}$$

is larger by a factor of $\sqrt{8/5}$, for n=2, than for the previous case in which z_0 was excluded. But, as in Section III*a*, for large n the enhancement factor F attains the asymptotic value of $\sqrt{2/3}$.

b. A Maximally Redundant ${}^nC_n$ Interferometer. To demonstrate that the degree of redundancy does not affect the sensitivity of an interferometer in an essential way, we consider here an array of n regularly spaced apertures in a one-dimensional geometry. There are $(n - 1)$ distinct spatial frequencies $\omega_0, 2\omega_0, \ldots, (n - 1)\omega_0$, where ω_0 is the spatial frequency of the baseline connecting two successive apertures. Clearly the spatial frequency $r\omega_0$ $(1 \le r \le n - 1)$ is $(n - r)$-fold redundant.

For simplicity, consider the case of a point source at the phase center. The average photoelectron count is given by

$$\langle k_p \rangle = \langle Q_0 \rangle \left[n + 2 \sum_{r=1}^{n-1} (n - r) \cos(pr\omega_0) \right] . \tag{3.11}$$

The fringe phasor z_r for spatial frequency $r\omega_0$ has the mean value

$$\langle z_r \rangle = \langle M \rangle (n - r) \tag{3.12}$$

We need to calculate the covariances of the real and imaginary parts of z_r to estimate the variance in the image. As before, we suppress the details of algebra and only present the final results for the map, made first without the zero spatial frequency and later with it. The results are at this stage still quite opaque and we, therefore, restrict even further to considering only the central pixel in the image.

(i) Inversion without Total Counts. At the phase center, the mean and variance are

$$I_5(0) = \langle C \rangle \frac{(n-1)}{2}, \tag{3.13}$$

$$V[i_5(0)] = \frac{\langle C \rangle}{12} [5n^2 - 9n + 4], \tag{3.14}$$

leading to an SNR at the phase center of amount

$$\frac{I_5(0)}{\sqrt{V[i_5(0)]}} = F \sqrt{\frac{\langle C \rangle}{2}}, \tag{3.15}$$

where $F = \sqrt{6n - 6/(5n - 4)}$ is our enhancement factor. For n=2 we find F=1 while the value of F in the limit of large n is $\sqrt{6/5}$.

(ii) True Inversion. Including the zero spatial frequency component in the Fourier inversion, we obtain the following mean and variance at the central pixel:

$$I_6(0) = \langle C \rangle \frac{n}{2}, \quad \text{and} \quad V[i_6(0)] = \frac{\langle C \rangle}{12} [5n^2 - 3n + 1], \tag{3.16}$$

Thus the SNR at the phase center is F $\sqrt{<(C>/2}$ where F, the enhancement factor, is

$$F = \sqrt{\frac{6n^2}{5n^2 - 3n + 1}} \quad . \tag{3.17}$$

For n=2, by including z_0 in the reconstruction process, F has been enhanced from 1 to $\sqrt{8/5}$. The limiting value of F for large n is $\sqrt{6/5.}$

In figure 1 we display our results for the enhancement factor F of the SNR as a function of the number of array elements for all six interferometers considered so far. What is most striking about the graph is that the SNR is more or less independent of the details of the array, whether it is ${}^nC_2$ or ${}^nC_n$ or whether it is redundant or not. The sensitivity of ideal Michelson interferometers is limited solely by the *total* number of photoelectrons detected by the *entire* array and not by how individual beams are combined on the detectors. Thus, if detectors are limited only by the photoelectron counting noise, then the sensitivity of an ${}^nC_r$ array should be qualitatively independent of r, the number of sub-beams per detector.

Section IV: An ${}^nC_2$ Ground-Based Array

A *direct* determination of the visibility phasors with ground-based synthetic aperture arrays is nearly impossible due to the phase corruption of the incident optical signals by the atmosphere. One must employ of closure-phase method of indirectly inferring the visibility data from estimators called variously as "triple products," "bispectra," etc. (Wirnitzer 1985, Baldwin *et al.* 1986). A bispectrum b refers to a set of three apertures, say i, j, k, and is defined as the product of the complex fringe phasors on the three baselines ij, jk, and ki that form the sides of the triangle with vertices i, j, k. The random phases contributed by the atmosphere at different apertures exactly cancel each other in the complex phase, the so called closure phase, of any such triple product.

We consider an ${}^nC_2$ array which has in all $n_t \equiv nC_3$ triple products only $n_b = {}^nC_2$ independent baselines. Thus not all triple products are independent. Furthermore, there is no analytical procedure by which the complex phasors can be exactly computed from the triple-product

data. There are iterative numerical schemes developed in the radio regime (Pearson and Readhead 1984), which may also be used in the optical regime to accomplish this approximately.

For a point source the only parameter that can be analytically inferred from the triple products is the source flux F. An estimate of F is $S^{1/3}$ where

$$S = \sum_{s=1}^{n_t} b_s \,. \tag{4.1}$$

We argue that the SNR of F is a good indicator of the SNR of the map inferred numerically from the bispectrum data. Clearly, the SNR of F is three times the SNR of S. In what follows, we restrict our discussions to a point source at the phase center of the array. For this case, all bispectra are equivalent just as all fringe phasors are.

To compute the SNR of F, we first compute the covariances of the individual triple products, b_s. Each b_s is correlated with itself as well as with the $3(n - 3)$ other triangles that share *one* side with it. Let σ_b^2 and $\mu\sigma_b^2$ represent the self-correlation (variance) and cross-correlation (covariance) of the bispectra. Then

$$\mathrm{SNR}(F) = \frac{3n_t \langle N \rangle^3}{\sqrt{n_t \sigma_b^2 + 3(n-3) n_t \mu\sigma_b^2}} \,, \tag{4.2}$$

where we have used the fact that all the fringe phasors are independent of one another for an ${}^nC_2$ array and each have the average value $\langle N \rangle$. It is not too hard to show (Kulkarni, Prasad, and Nakajima *in preparation*) that

$$\sigma_b^2 = 6\langle N \rangle^5 + 12\langle N \rangle^4 + 8\langle N \rangle^3 \text{ and } \mu\sigma_b^2 = 2\langle N \rangle^5. \tag{4.3}$$

Thus the final expression of SNR (F) is

$$\mathrm{SNR}(F) = \frac{3\sqrt{n_t}\langle N \rangle^3}{\sqrt{6(n-2)\langle N \rangle^5 + 12\langle N \rangle^4 + 8\langle N \rangle^3}} \tag{4.4}$$

(i) High-Photon-Number Limit: $<N>>>1$. The SNR of the measured source strength tends in the limit $<N>>>1$ to the value $\sqrt{<C>/2}$. This is essentially the same SNR as attainable in ideal imaging considered in Section II*a*. Thus, in the high-photon-number limit, imaging sensitivity is limited solely by the total photon number intercepted by the array, not by the details of the imaging algorithm.

(ii) Low-Photon-Number Limit. $<N><<1$. For very weak source strengths, the SNR of F tends to the value $\sqrt{9n(n-1)(n-2)<N>^3/48}$. In terms of the $<M>$, the number of photons per primary beam, ($<N>=<M>/(n-1)$) this expression reduces to $3<M>^{3/2}/\sqrt{48}$ for a large number n of apertures. In this double limit, therefore, the SNR depends only on the number of photons collected by a *single* aperture and not by the entire array.

Nakajima (1988) has shown that if the primary beams are not split and recombined, then the SNR of F is much greater than the preceding result at low photon numbers. Thus, at low photon numbers, beam splitting is a distinct detriment to the sensitivity of ground-based interferometers using the closure-phase method of triple products.

Section V: Discussion

In this work, we have studied the dependence of the sensitivity and of the distribution of noise across the image plane of an optical interferometer on the details of beam splitting and recombination. Of the many possibilities, we have studied two extreme cases: *(i)* the so called ${}^nC_2$ interferometer in which the beam from each element is split equally into n-1 sub-beams and the resulting $n(n-1)$ sub-beams combined pair-wise onto $n_b = {}^nC_2$ detectors and *(ii)* an ${}^nC_n$ interferometer in which all the beams are combined on one detector. Our most important result is that up to factors of order 1 the SNR in the *directly* synthesized image for either kind of array is equal to $\sqrt{<L>/2}$ where $<L>$ is the total number of photoelectrons collected by the array. Thus the beam combination geometry should *not* be a critical issue in the design of a space interferometer.

Direct synthesis is not possible for ground-based arrays that suffer from atmospheric phase aberrations, and one must use the closure-phase method of *indirect* computation of the visibility data. We have looked at a nominal SNR for measurements from an ${}^nC_2$ array and found the physically reasonable result that at high photon numbers both direct and indirect imaging are

equally sensitive. However, at low photon numbers the sensitivity depends only on the photon number collected by each aperture and not by the entire array.

This work was done entirely in collaboration with S.R. Kulkarni at Caltech, who had most of the early ideas.

References

1. Baldwin, J. E; Haniff, C.A.; Mackay, C.D.; Warner, P.J. 1986. *Nature* 320:595.

2. Goodman, J.W. 1985. *Statistical Optics*, (Wiley:New York).

3. Kulkarni, S.R. 1989. *sub. to Astron. J.*

4. Kulkarni, S.R.; Prasad, S.; Nakajima, T. *in preparation.*

5. Nakajima, T. 1988. *J. Opt. Soc. Am.* A5:1477

6. Pearson, T.J.; Readhead, A.C.S. 1984. *Annu. Rev. Astron. Astrophys.* 22:97.

7. Perley, R.A.; Schwab, F.R.; Bridle, A.H. 1985. *Synthesis Imaging*, (NRAO:Socorro).

8. Prasad, S; Kulkarni, S.R. 1989. *J. Opt. Soc. Am.* A6:1702.

9. Wirnitzer, B. 1985, *J. Opt. Soc. Am.* A2:14.

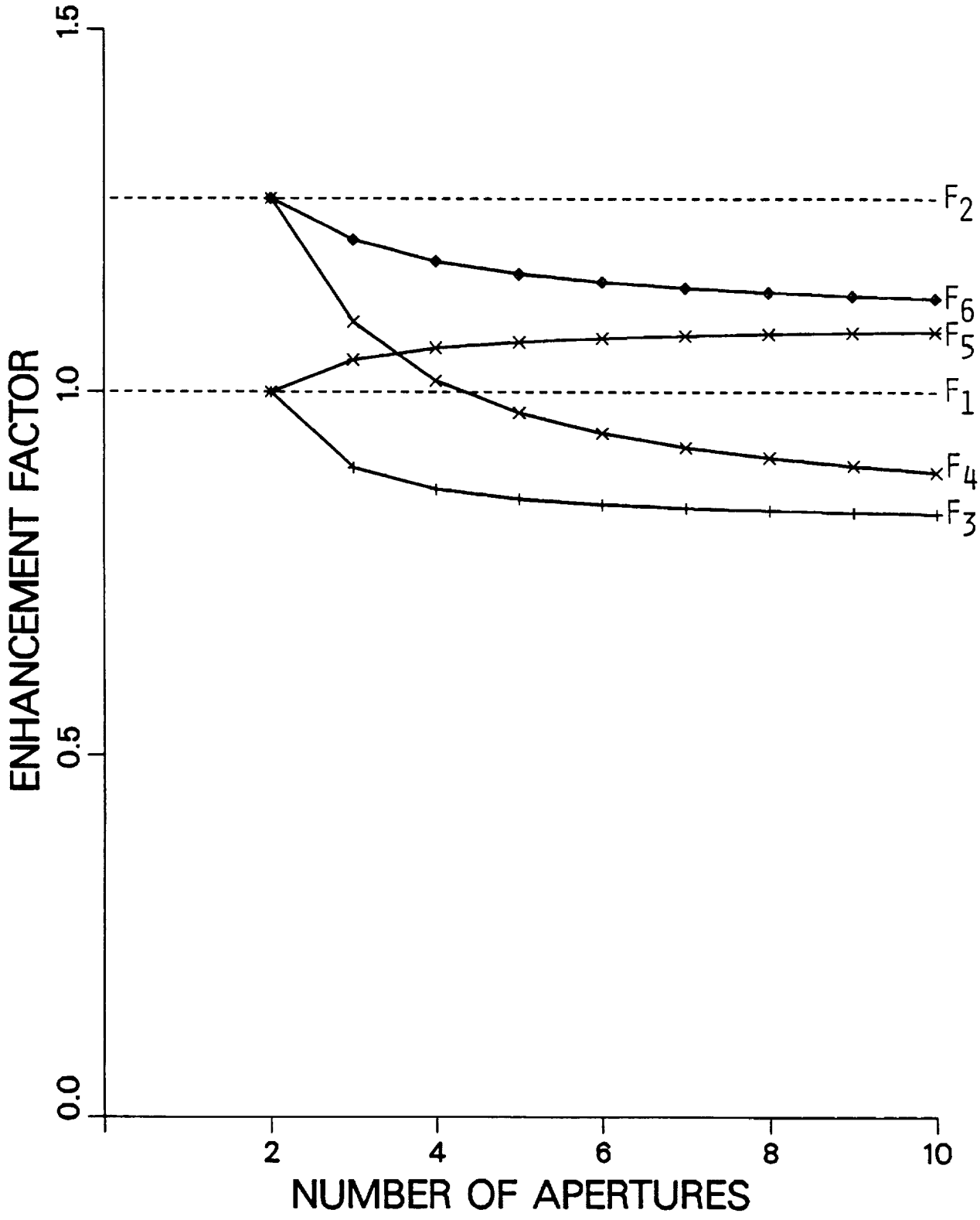

Figure 1: Enhancement factor F of SNR versus the number n of apertures in the array. F_1 and F_2 refer to the ${}^nC_2$ array without and with the zero frequency, F_3 and F_4 refer to the nonredundant ${}^nC_n$ array, and F_5 and F_6 refer to the maximally redundant ${}^nC_n$ array.

PART III

SPACE-BASED INTERFEROMETERS

This section of the proceedings is devoted to discussions of recent proposals for Earth-orbiting optical/IR interferometers. Before building a long-baseline optical interferometer on the Moon, we must first gain experience on short-baseline arrays in space. These papers describe innovative ideas for orbiting interferometers, the technical challenges, and the science drivers.

M. Shao begins with a brief discussion of the technical requirements and performance of a first-generation space interferometer, with particular emphasis on OSI, a project for the Space Station. Pierre Bely and colleagues next describe HARDI, a high-angular-resolution deployable interferometer for space, that will have a 6-meter baseline and thus greatly improve the resolution of the Hubble Space Telescope (HST). The support and servicing of large observatories in space, based on experience with HST, is summarized by T.E. Styczynski. The final paper by S.T. Ridgway serves as a bridge between Parts III and IV of these proceedings by describing the science drivers and technical requirements for interferometers in Earth-orbit and on the Moon.